Short Communication

Electrochemical Deposition of Calcium Phosphate/Chitosan/Gentamicin on a Titanium Alloy for Bone Tissue Healing

Shailin Zhang[#], Xiangyu Cheng[#], Jixiang Shi, Jinhui Pang, Zhen Wang, Wenjun Shi, Fuying Liu and Bin Ji[*]

Department of Orthopaedics, Putuo Hospital, Shanghai University of Traditional Chinese Medicine, Shanghai, 200062, China
Department of Orthopedics, Putuo Hospital, Shanghai University of Traditional Chinese Medicine, 164 Lanxi Road, Shanghai 200062, China
E-mail: binjikatelly@sina.com
[#] These authors contributed equally to the work.

In the present study, a calcium phosphate/chitosan/gentamicin (Ca-P/CS/gentamicin) film was deposited onto a titanium alloy surface through electrochemical deposition. High drug loading into the coating was described, along with a controlled release of the drug over two days. After the implantation of the developed film into rat calvarial defects, new woven bone was formed in the defects and mineralized at a high rate (62.5 mm/day) during the initial stages, which is much higher than that of normal bone growth rates (several mm/day, 0.1 mg/day).

1. INTRODUCTION

Due to their degradable properties, titanium and related alloys have advantages over other alloys such as stainless steel [1-5]. Therefore, titanium and related alloys have been accepted as more favourable materials for implantation into the human body. Unfortunately, these alloys also exhibit certain disadvantages, including undesirable corrosion resistance and high chemical activity [6-10]. In corrosive media (pH < 11.5 or Cl-containing media), the corrosion rates of titanium-based materials are faster [11]. Previous studies investigated the corrosion resistance of a medical AZ91 Mg alloy in a simulated solution [12, 13], and the results have shown a fast degradation in the titanium alloy soaked

in the simulated solution during the earlier stage. Additionally, in a physiological environment containing Cl, the use of titanium could lead to the formation of amorphous degradation products and porous pitted surfaces. Therefore, the use of titanium and related alloys can affect the surrounding tissue during the early implantation stage. To improve material histocompatibility, it is essential to control the degradation rate and enhance the biological activity [14, 15]. Through titanium alloy surface modification, the corrosion rate and implant material biocompatibility of the alloy can be improved, and its degradation rate can also be adjusted to the bone healing speed.

Gentamicin, an antibiotic of the aminoglycoside family, has gained wide application recently. Many previous studies have employed a wide range of coatings and loading routes to study the gentamicin release involved in antibacterial implants [3, 16-20]. Lucke and coworkers [21] investigated the gentamicin-loaded poly(D,L-lactide) coating on a metallic implant in a rat model. Price and coworkers [22, 23] presented the transportation of gentamicin through a biodegradable carrier, namely, a polylactic-co-glycolic acid copolymer. Pishbin and coworkers [22] described the electrophoretic deposition of a chitosan (CS)-bioactive glass composite containing gentamicin. Hayes et al. and Van de Belt et al. [24, 25] proposed a coating that eluted antibiotics for sixty days (40% of the elution occurred during the initial five days).

The present study reports the preparation of antibiotics involving Ca-P/CS composite films deposited using an electrochemical process. The optimization of different parameters on the synthesis of the composite materials was also determined based on a systematic investigation. The composite film was developed to heal large bone defects that are unable to self-heal and require a relatively large bone graft as an artificial bone substitute. A critical-sized defect (CSD) refers to the minimal defect that will not heal, regardless of the healing time.

2. EXPERIMENTS

2.1. Chemicals

Commercially available gentamicin sulfate, dextran sulfate, acetic acid, pentasodium tripolyphosphate hexahydrate (TPP), low-molecular-weight CS, nitric acid (65%), hydrofluoric acid (40%), ammonium dihydrogen phosphate (98%), calcium nitrate (99%), sodium hydroxide (analytical grade), sodium borate, o-phthaldialdehyde, phosphate buffered saline (PBS), and 2-mercaptoethanol were acquired from Sigma-Aldrich. Hydrochloric acid and isopropanol were both of analytical grade and were commercially available from Bio-Lab. The Ti-6Al-4V ELI grade rods (length, 5 mm; diameter, 9.5 mm) were produced by Dynamet Technology Inc. and supplied by Barmil. The disks were used as the working electrode in our case. Deionized (DI) water (>18 MV cm) was used throughout the experiments.

2.2. Synthesis of the compound CS/gentamicin nanoparticles

The synthesis of the CS nanoparticles was based on the ionic cross-linking of CS with TPP. For the preparation of a 0.2% CS solution (w/v), CS was dissolved in 1% diluted acetic acid (v/v) under

sonication at ambient temperature. The obtained CS solution (pH range: 4.0 - 5.5) was then flush mixed with a specific volume of the SA and GM solution. This step was followed by the dropwise addition of the gentamicin-dextran sulfate mixture under magnetic stirring for 60 s at 1000 rpm. Under the same conditions, 10 mL of TPP (0.8% w/v) was also dropwise added into the as-prepared mixture, upon which the CS nanoparticles were formed. After continuous stirring for 60 min, the obtained nanoparticle suspensions were centrifuged for 0.5 h at 16,000 rpm. In addition, the final nanoparticle products were lyophilized and stored before use.

2.3. Electrodeposition

Based on a Ca-P molar ratio of 1.67, the electrodeposition solution containing CS–acetic acid (4%), $NH_4H_2PO_4$ (0.025 M), gentamicin/CS (1 mg/mL), and $Ca(NO_3)2H_2O$ (0.042 M) was synthesized. Initially, $Ca(NO_3)_2$ and CS–acetic acid were added into the electrolytic assembly, followed by the slow addition of $NH_4H_2PO_4$ under stirring. Then, the alloy was immersed into the as-prepared mixed solution for electrodeposition. The effects of various CS contents, deposition times, deposition temperatures, and current densities on the performance of the as-prepared Ca-P/CS/gentamicin films were investigated. Finally, the optimum film was cultured in simulated body fluid (SBF) to study its mineralization performance. The reagents for the preparation of SBF are summarized in Table 1.

Table 1. Reagents for the preparation of SBF (pH 7.40, 1 L).

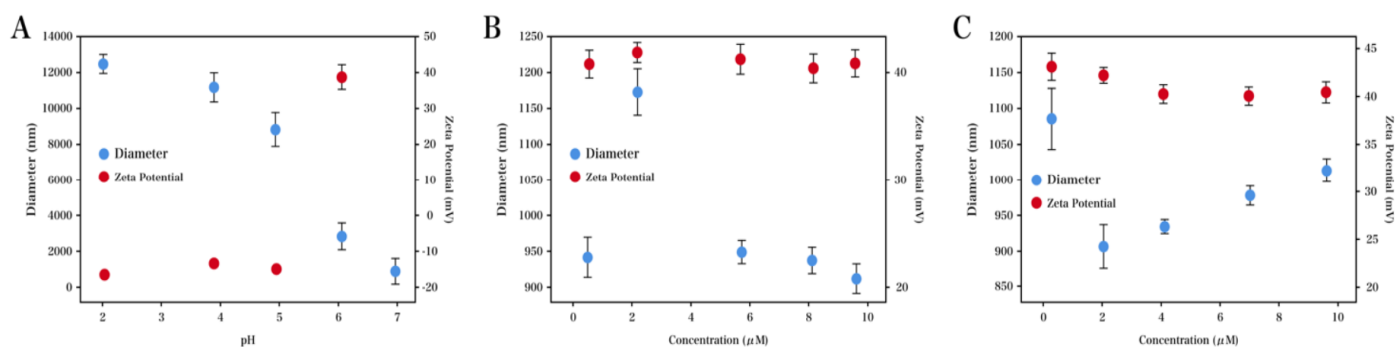| Order	Reagent	Amount
1	NaCl	7.996 g
2	$NaHCO_3$	0.350 g
3	KCl	0.224 g
4	K_2HPO_4	0.228 g
5	$MgCl_2$	0.305 g
6	1M-HCl	40 mL
(About 90 % of total amount of HCl to be added)		
7	$CaCl_2$	0.278 g
8	Na_2SO_4	0.071 g
9	$(CH_2OH)_3CNH_2$	6.057 g

2.4 Characterizations

A Rigaku Rotalflex RU-200B diffractometer equipped with a Ni filter and a Cu Kα (λ = 1.5418 Å) source operating at 40 kV and 40 mA was used for a crystallographic investigation. The zeta measurements were carried out using a Zetasizer system (Model ZEN 3600, Malvern Instruments, Malvern, UK). The potentiodynamic polarization measurements were performed using a conventional

three-electrode setup in SBF. All the potentiodynamic polarization tests were performed at a scan rate of 1 mV/s. The analysis of gentamicin was carried out using UV-Vis spectroscopy *via* a Halo RB-10 UV-Vis spectrophotometer.
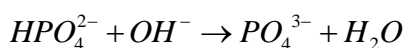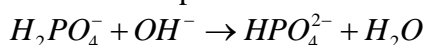

3. RESULTS AND DISCUSSION

The amount of gentamicin in the as-prepared NPs was set as 67% (wt.%). Figure 1 shows the influences of pH and ionic species (such as P and Ca in the suspension) on the size and ζ-potential of the NPs. Considering the CS pK of approximately 6.3, the ζ-potential is expected to be positive when the pH is lower than the pK, and a further increase in pH will lead to a lower ζ-potential [26]. Therefore, aggregation occurs when the pH exceeds the pK, as shown from the particle size results. In the case of an acidic pH, the NPs show a smaller diameter and a higher zeta potential, which suggest a stable suspension. The suspension remained stable at all concentrations, and the NPs were only slightly enlarged compared with their original sizes. It can be seen that the NPs may be precipitated in an acidic solution in an electrochemical system, where negative potentials are applied, which lead to water reduction and an increase in pH near the working electrode. This phenomenon was consistent with the electrochemical deposition of Ca-P, also realized by an increase in the electrochemical pH [27, 28]. These results indicate that when water in a suspension contained both ionic species of P and Ca, CS/gentamicin NPs were electrochemically reduced, and the two species were simultaneously deposited.
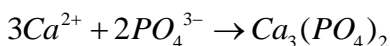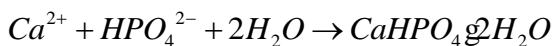

Figure 1. Optimization of parameters: (A) pH effect on the size and zeta potential of drug-loaded particles in suspension; (B) solution Ca concentration effect on the diameter and zeta potential of drug-loaded particles in suspension; and (C) Ca-P effect on the diameter and zeta potential of drug-loaded NPs in suspension.
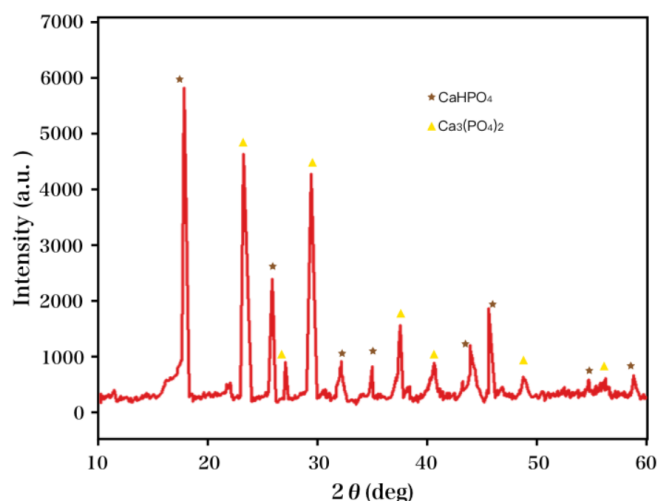
The electrodeposition mechanism in an electrolyte containing chitosan is described as follows:

$$H_2PO_4^- + OH^- \rightarrow HPO_4^{2-} + H_2O$$

$$HPO_4^{2-} + OH^- \rightarrow PO_4^{3-} + H_2O$$

CaHPO$_4$ 2H$_2$O (DCPD) or Ca$_3$(PO$_4$)$_2$ were formed after OH was adsorbed on the cathode in the presence of Ca^{2+} and H$_2$PO$_4^-$ in the electric field:

$$Ca^{2+} + HPO_4^{2-} + 2H_2O \rightarrow CaHPO_4 \cdot 2H_2O$$
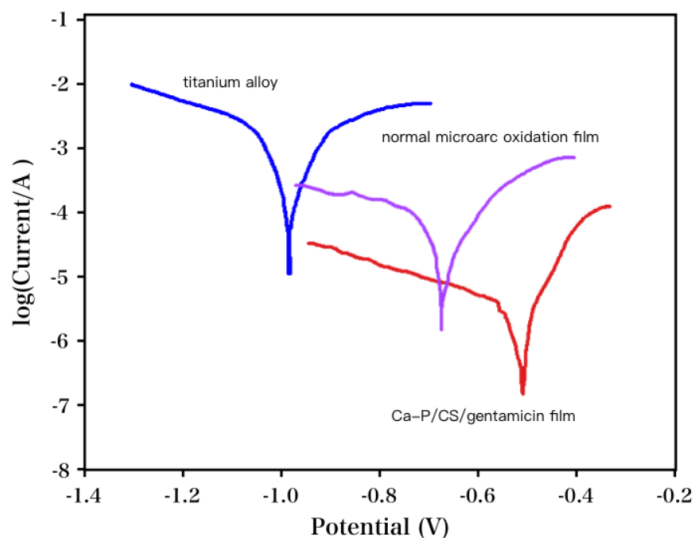$$3Ca^{2+} + 2PO_4^{3-} \rightarrow Ca_3(PO_4)_2$$

The optimized parameters for the preparation of the Ca-P/CS/gentamicin film are as follows: current density, 3 mA/cm^2; deposition time, 0.5 h; deposition temperature, 30°C; added CS/gentamicin volume, 3 mL, as shown in the XRD pattern of Figure 2. Additionally, the diffraction peaks of CaHPO$_4$·2H$_2$O (DCPD) and Ca$_3$(PO$_4$)$_2$ were also observed. Furthermore, the diffraction peaks of TCP were observed in the vicinity of 33°, 45°, and 60°, and the diffraction peaks of DCPD appeared over a range of 10° and 35°.

Figure 2. XRD patterns recorded for the Ca-P/CS/gentamicin film synthesized under optimum parameters (30°C, 3 mL chitosan, 3 mA/cm^2 and 30 min).
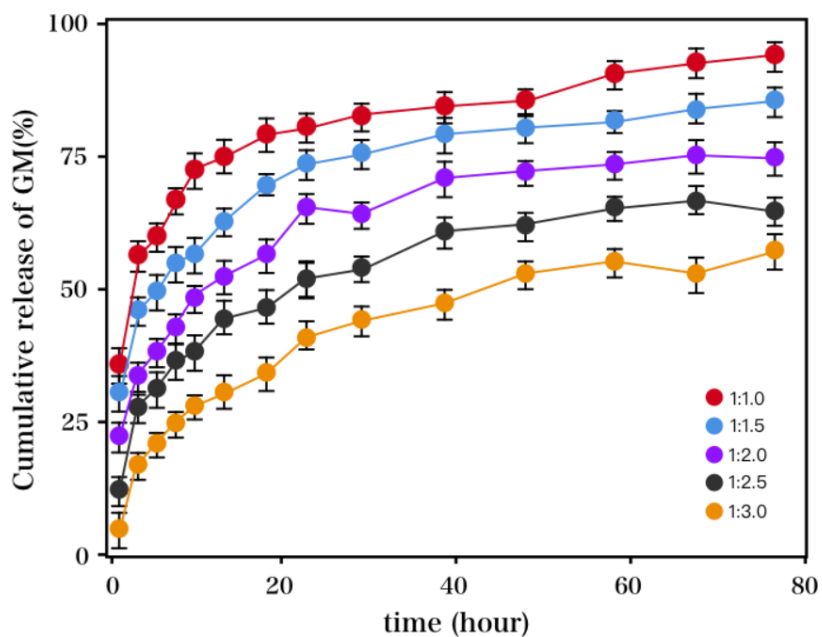
For the titanium alloy, the dynamic polarization curves for both the normal microarc oxidation and Ca-P/CS/gentamicin films in SBF are shown in Figure 3. For the normal microarc oxidation-treated titanium alloy, the corrosion potentials showed a clear shift from -1.0 V to -0.64 V due to the surface passivation process. Therefore, the normal microarc oxidation can be considered an effective method for titanium alloy treatment. For the Ca-P/CS/gentamicin film, the corrosion potential shifted in the positive direction approximately 400 mV and 100 mV when compared with the matrix and the microarc oxidation membrane of the titanium alloy, respectively. However, the size of passivation regions and their corresponding stable current density varied. On the other hand, the thin Ca-P/CS/gentamicin film showed a sharply decreased corrosion current, suggesting more favourable anticorrosion behaviour. Therefore, it can be concluded that the biological film was suitable for the substrate in SBF. Table 2 shows the polarization parameters of the substrate, normal microarc oxidation film and Ca-P/CS/gentamicin film in SBF. When the potential increased as high as -521 mV, the Ca-P/CS/gentamicin film showed no breakdown potential, indicating that this sample was highly resistant to local corrosion.

Figure 3. Polarization curves recorded for the substrate, normal microarc oxidation film and Ca-P/CS/gentamicin film in SBF.

Table 2. Electrochemical polarization parameters for the substrate, normal microarc oxidation film and Ca-P/CS/gentamicin film in SBF.

Sample	E_{corr} (mV)	b_a (mV/dec)	b_c (mV/dec)
Titanium alloy	-1007	85	97
Normal microarc oxidation film	-644	84	102
Ca-P/CS/gentamicin film	-521	78	97

Figure 4. *In vitro* release profile recorded for gentamicin from the Ca-P/CS/gentamicin film with varying feed ratios of CS to gentamicin (n = 3).

Figure 4 shows the *in vitro* cumulative release of gentamicin from our developed film with varying feed ratios of CS to gentamicin over a range of 1.0:1.0 to 3.0:10. The corresponding release profile exhibited three phases [29]: an initial rapid release phase, a relatively slow release phase, and an even slower release phase. The rapid release (within the first 4 h) can also be referred to as a burst release. In brief, approximately 46% gentamicin was released (feed ratio of CS:gentamicin, 2.0:1.0). This process mainly results from the simple diffusion of the nanoparticles on the surface during the first phase. The following phase (4 to 12 h) was due to the diffusion of these drugs from the matrix, where approximately 87% gentamicin was released. The last phase resulted from the degradation of the polymer, which was characterized by the diffusion of the dissolved drugs into the release medium. From the compound nanoparticles, the cumulative percentage release of gentamicin reached approximately 95% (in 72 h). The formulations with a higher amount of drugs showed a higher drug release rate, whilst those with a lower amount of drugs exhibited a lower release rate [30]. Since the antibiotic is highly soluble, it can be hypothesized that either the drug is not exposed to the aqueous environment or there is a diffusion barrier inside the coating. This encapsulation may be beneficial if the barriers can be removed during the late stages of implantation, allowing the remainder of the drug to elute.

The synergistic effects of the physical factors (the degradation rate of the implanted biomaterials, availability of bone minerals, physical scaffolds, etc.) and biological factors (anatomic position, age, species, etc.) determine the bone healing kinetics. As shown in the histological studies, by day 40, new bone was almost completely substituted for the biomaterial during the repair of rat CSDs. Given that the bone was growing at a nominally constant rate, the average growing speed of the bone was calculated to be 2.5 mm/40 days, i.e., 62.5 mm/day, which is significantly higher than that of conventional bone remodelling for rats of the same age [31]. For the 4-month-old rats, the obtained bone growth rate was low, i.e., only several mm/day [32].

4. CONCLUSIONS

The present study reported the successful deposition of Ca-P/CS/gentamicin films onto a titanium alloy surface under optimum conditions. It was found from the *in vitro* release profile that the release rate of gentamicin from the developed films was affected by the feed ratio. The developed films enhanced the bone growth rate of the defects at the initial stage, showing a growth rate of 62.5 mm/day, which is significantly higher than that of the growth rate of normal bone.

References

1. A.Arifin, A.B. Sulong, N. Muhamad, J. Syarif and M.I. Ramli, *Materials & Design*, 55 (2014) 165.

2. X. Li, X.Y. Ma, Y.F. Feng, Z.S. Ma, J. Wang, T.C. Ma, W. Qi, W. Lei and L. Wang, *Biomaterials*, 36 (2015) 44.
3. M. Diefenbeck, C. Schrader, F. Gras, T. Mückley, J. Schmidt, S. Zankovych, J. Bossert, K.D. Jandt, A. Völpel and B.W. Sigusch, *Biomaterials*, 101 (2016) 156.
4. A.Y. Wu, J.T. Hsu and H.L. Huang, *Implant Dentistry*, 23 (2014) 534.
5. T.J. Lee, T. Ueno, N. Nomura, N. Wakabayashi and T. Hanawa, *International Journal of Oral & Maxillofacial Implants*, 31 (2016) 547.
6. W.E.G. Müller, E. Tolba, H.C. Schröder, S. Wang, G. Glasser, B. Diehl-Seifert and X. Wang, *Rsc Advances*, 5 (2015) 75465.
7. B.H. Wu, S. Chen, J. Wu, Y.X. Leng, D. Xie, F. Jiang, N. Huang and H. Sun, *Surface & Coatings Technology*, 277 (2015) 197.
8. L. Rui, K. Memarzadeh, C. Bei, Y. Zhang, M. Zheng, R.P. Allaker, R. Ling and Y. Ke, *Scientific reports*, 6 (2016) 29985.
9. H. Minamikawa, T. Ikeda, W. Att, Y. Hagiwara, M. Hirota, M. Tabuchi, H. Aita, W. Park and T. Ogawa, *Journal of Biomedical Materials Research Part A*, 102 (2014) 3618.
10. B. Ganesh, W. Sha, N. Ramanaiah and A. Krishnaiah, *Materials & Design*, 56 (2014) 480.
11. C. Caparrós, J. Guillem-Martí, M. Molmeneu, M. Punset, J.A. Calero and F.J. Gil, *Journal of the Mechanical Behavior of Biomedical Materials*, 39 (2014) 79.
12. S.V. Gnedenkov, Y.P. Sharkeev, S.L. Sinebryukhov, O.A. Khrisanfova, E.V. Legostaeva, A.G. Zavidnaya, A.V. Puz', I.A. Khlusov and D.P. Opra, *Corrosion Reviews*, 34 (2016) 65.
13. A. Rodríguez-Cano, M.Á. Pacha-Olivenza, R. Babiano, P. Cintas and M.L. González-Martín, *Surface & Coatings Technology*, 245 (2014) 66.
14. J. Xu, L. Liu, P. Munroe and Z.H. Xie, *Journal of Materials Chemistry B*, 3 (2015) 4082.
15. J. Cabrera-Domínguez, L. Castellanos-Cosano, D. Torres-Lagares and G. Machuca-Portillo, *International Journal of Oral & Maxillofacial Implants*, 32 (2017) 1135.
16. B. Thomas, D. Kulichova, R. Wolf, B. Summer, V. Mahler and P. Thomas, *Contact Dermatitis*, 73 (2016) 343.
17. J. Pochhammer, S. Zacheja and M. Schäffer, *Langenbecks Archives of Surgery*, 400 (2015) 1.
18. S. Nast, M. Fassbender, N. Bormann, S. Beck, A. Montali, M. Lucke, G. Schmidmaier and B. Wildemann, *Journal of Biomaterials Applications*, 31 (2016) 45.
19. Q. Liu, Z. Zhou, W. Lu, L. Zhou and J. Tao, *Journal of Biomaterials & Tissue Engineering*, 6 (2016) 390.
20. C. Flores, S. Degoutin, F. Chai, G. Raoul, J.C. Hornez, B. Martel, J. Siepmann, J. Ferri and N. Blanchemain, *Materials Science & Engineering C Materials for Biological Applications*, 64 (2016) 108.
21. M. Lucke, G. Schmidmaier, S. Sadoni, B. Wildemann, R. Schiller, N.P. Haas and M. Raschke, *Bone*, 32 (2003) 521.
22. F. Pishbin, V. Mouriño, S. Flor, S. Kreppel, V. Salih, M.P. Ryan and A.R. Boccaccini, *ACS applied materials & interfaces*, 6 (2014) 8796.
23. J.S. Price, A.F. Tencer, D.M. Arm and G.A. Bohach, *Journal of Biomedical Materials Research*, 30 (1996) 281.
24. G. Hayes, N. Moens and T. Gibson, *Veterinary & Comparative Orthopaedics & Traumatology V.c.o.t*, 26 (2013) 251.
25. d.B.H. Van, D. Neut, W. Schenk, J.R. van Horn, V.D.M. Hc and H.J. Busscher, *Acta Orthopaedica Scandinavica*, 72 (2001) 557.
26. T. Danieli and D. Mandler, *Journal of Solid State Electrochemistry*, 17 (2013) 2989.
27. N. Eliaz and T. Sridhar, *Crystal Growth and Design*, 8 (2008) 3965.
28. N. Metoki, L. Leifenberg-Kuznits, W. Kopelovich, L. Burstein, M. Gozin and N. Eliaz, *Mater. Lett.*, 119 (2014) 24.
29. S.A. Agnihotri and T.M. Aminabhavi, *Journal of Controlled Release*, 96 (2004) 245.

30. A.P. Rokhade, N.B. Shelke, S.A. Patil and T.M. Aminabhavi, *Carbohydrate Polymers*, 69 (2007) 678.
31. L.I. Hansson, K. Menander-Sellman, A. Stenström and K.G. Thorngren, *Calcified Tissue Research*, 10 (1972) 238.
32. A. Raman, *Acta Orthopaedica Scandinavica*, 40 (1969) 193.